

---

# Dynamic Filter Networks

---

**Bert De Brabandere**<sup>1\*</sup>  
ESAT-PSI, KU Leuven

**Xu Jia**<sup>1\*</sup>  
ESAT-PSI, KU Leuven, iMinds

**Tinne Tuytelaars**<sup>1</sup>  
ESAT-PSI, KU Leuven, iMinds

**Luc Van Gool**<sup>1,2</sup>  
ESAT-PSI, KU Leuven  
D-ITET, ETH Zurich

<sup>1</sup>firstname.lastname@esat.kuleuven.be    <sup>2</sup>vangool@vision.ee.ethz.ch

## Abstract

In a traditional convolutional layer, the learned filters stay fixed after training. In contrast, we introduce a new framework, the *Dynamic Filter Network*, where filters are generated dynamically conditioned on an input. We show that this architecture is a powerful one, with increased flexibility thanks to its adaptive nature, yet without an excessive increase in the number of model parameters. A wide variety of filtering operations can be learned this way, including local spatial transformations, but also others like selective (de)blurring or adaptive feature extraction. Moreover, multiple such layers can be combined, e.g. in a recurrent architecture.

We demonstrate the effectiveness of the dynamic filter network on the tasks of video and stereo prediction, and reach state-of-the-art performance on the moving MNIST dataset with a much smaller model. By visualizing the learned filters, we illustrate that the network has picked up flow information by only looking at unlabelled training data. This suggests that the network can be used to pretrain networks for various supervised tasks in an unsupervised way, like optical flow and depth estimation.

## 1 Introduction

Humans are good at predicting another view from related views. For example, humans can use their everyday experience to predict how the next frame in a video will differ; or after seeing a person's profile face have an idea of her frontal view. This capability is extremely useful to get early warnings about impinging dangers, to be prepared for necessary actions, etc. The vision community has realized that endowing machines with similar capabilities would be rewarding.

Several papers have already addressed the generation of an image conditioned on given image(s). Yim *et al.* [25] and Yang *et al.* [24] learn to rotate a given face to another pose. The authors of [18, 21, 20, 17, 14] train a deep neural network to predict subsequent video frames. Flynn *et al.* [5] use a deep network to interpolate between views separated by a wide baseline. Yet all these methods apply the exact same set of filtering operations on each and every input image. This seems suboptimal for the tasks at hand. For example, for video prediction, there are different motion patterns within different video clips. The main idea behind our work is to generate the future frames with parameters adapted to the motion pattern within a particular video. Therefore, we propose a learnable parameter layer that provides custom parameters for different samples.

---

\*X. Jia and B. De Brabandere contributed equally to this work and listed in alphabetical order.

Our *dynamic filter module* consists of two parts: a *filter-generating network* and a *dynamic filtering layer* (see Figure 1). The filter-generating network dynamically generates sample-specific filter parameters conditioned on the network’s input. Note that these are not fixed after training, like regular model parameters. The dynamic filtering layer then applies those sample-specific filters to the input. Both components of the dynamic filter module are differentiable with respect to the model parameters such that gradients can be backpropagated throughout the network. The filters can be convolutional, but other options are possible. In particular, we propose a special kind of dynamic filtering layer which we coin *dynamic local filtering layer*, which is not only sample-specific but also position-specific. The filters in that case vary from position to position and from sample to sample, allowing for more sophisticated operations on the input. Our framework can learn both spatial and photometric changes, as pixels are not simply displaced, but the filters possibly operate on entire neighbourhoods.

We demonstrate the effectiveness of the proposed dynamic filter module on several tasks, including video prediction and stereo prediction. We also show that, because the computed dynamic filters are explicitly calculated - can be visualised as an image similar to an optical flow or stereo map. Moreover, they are learned in a totally unsupervised way, i.e. without groundtruth maps.

The rest of paper is organised as follows. In section 2 we discuss related work. Section 3 describes the proposed method. We show the evaluation in section 4 and conclude the paper in section 5.

## 2 Related Work

**Deep learning architectures** Several recent works explore the idea of introducing more flexibility into the network architecture. Jaderberg *et al.* [11] propose a module called Spatial Transformer, which allows the network to actively spatially transform feature maps conditioned on themselves without explicit supervision. They show this module is able to perform translation, scaling, rotation and other general warping transformations. They apply this module to a standard CNN network for classification, making it invariant to a set of spatial transformations. This seminal method only works with parametric transformations however, and applies a single transformation to the entire feature map(s). Patraucean *et al.* [17] extend the Spatial Transformer by modifying the grid generator such that it has one transformation for each position, instead of a single transformation for the entire image. They exploit this idea for the task of video frame prediction, applying the learned dense transformation map to the current frame to generate the next frame. Similarly, our method also applies a position specific transformation to the image or feature maps and takes video frame prediction as one testbed. In contrast to that work, our method generates the new image by applying dynamic local filters to the input image or feature maps instead of using a grid generator and sampler. Our method is not only able to learn how to displace a pixel, but how to construct it from an entire neighborhood, including its intensity (e.g. by learning a blur kernel).

In the context of visual question answering, Noh *et al.* [15] introduce a dynamic parameter layer whose output is used as parameters of a fully connected layer. In that work, the dynamic parameter layer takes the information from another domain, *i.e.* question representation, as input. They further apply hashing to address the issue of predicting the large amount of weights needed for a fully connected layer. Different from their work, we propose to apply the dynamically generated filters to perform a filtering operation on an image, hence we do not have the same problem of predicting large amounts of parameters. Most similar to our work, a dynamic convolution layer is proposed by Klein *et al.* in [13] in the context of short range weather prediction and by Riegler *et al.* in [19] for single image non-blind single image super resolution. Our work differs from theirs in that it is more general: dynamic filter networks are not limited to translation-invariant convolutions, but also allow position-specific filtering using a dynamic locally connected layer.

**New view synthesis** Our work is also related to works on new view synthesis, that is, generating a new view conditioned on the given views of a scene. One popular task in this category is to predict future video frames. Ranzato *et al.* [18] use an encoder-decoder framework in a way similar to language modeling. Srivastava *et al.* [21] propose a multilayer LSTM based autoencoder for both past frames reconstruction and future frames prediction. This work has been extended by Shi *et al.* [20] who propose to use convolutional LSTM to replace the fully connected LSTM in the network. The use of convolutional LSTM reduces the amount of model parameters and also exploits the local correlation in the image. Oh *et al.* [16] address the problem of predicting future frames conditioned

on both previous frames and actions. They propose the encoding-transformation-decoding framework with either feedforward encoding or recurrent encoding to address this task. Mathieu *et al.* [14] manage to generate reasonably sharp frames by means of a multi-scale architecture, an adversarial training method, and an image gradient difference loss function. In a similar vein, Flynn *et al.* [5] apply a deep network to produce unseen views given neighboring views of a scene. Their network comes with a selection tower and a color tower, and is trained in an end-to-end fashion. This idea is further refined by Xie *et al.* [23] for 2D-to-3D conversion. None of these works adapt the filter operations of the network to the specific input sample, as we do, with the exception of [5, 23]. We’ll discuss the relation between their selection tower and our dynamic filter layer in section 3.3.

**Shortcut connections** Our work also shares some similarity, through the use of shortcut connections, with the highway network [22] and the residual network [8, 10]. For a module in the highway network, the transform gate and the carry gate are defined to control the information flow across layers. Similarly, He *et al.* [8, 10] propose to reformulate layers as learning residual functions instead of learning unreferenced functions. Compared to the highway network, residual networks remove the gates in the highway network module and the path for input is always open throughout the network. In our network architecture, we also learn a referenced function. Yet, instead of applying addition to the input, we apply filtering to the input - see section 3.3 for more details.

### 3 Dynamic Filter Networks

In this section we describe our dynamic filter framework. A dynamic filter module consists of a filter-generating network that produces filters conditioned on an input, and a dynamic filtering layer that applies the generated filters to another input. Both components of the dynamic filter module are differentiable. The two inputs of the module can be either identical or different, depending on the task. The general architecture of this module is shown schematically in Figure 1. We explicitly model the transformation: invariance to change should not imply one becomes totally blind to it. Moreover, such explicit modeling allows unsupervised learning of transformation fields like optical flow or depth.

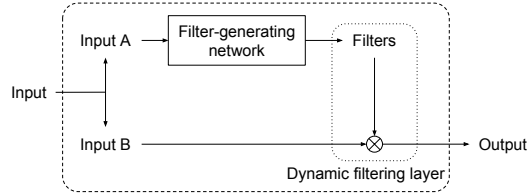


Figure 1: The general architecture of a Dynamic Filter Network.

For clarity, we make a distinction between *model parameters* and *dynamically generated parameters*. Model parameters denote the layer parameters that are initialized in advance and only updated during training. They are the same for all samples. Dynamically generated parameters are sample-specific, and are produced on-the-fly without a need for initialization. The filter-generating network outputs dynamically generated parameters, while its own parameters are part of the model parameters.

#### 3.1 Filter-Generating Network

The filter-generating network takes an input  $I_A \in \mathbb{R}^{h \times w \times c_A}$ , where  $h$ ,  $w$  and  $c_A$  are height, width and number of channels of the input  $A$  respectively. It outputs filters  $\mathcal{F}_\theta$  parameterized by parameters  $\theta \in \mathbb{R}^{s \times s \times c_B \times n \times d}$ , where  $s$  is the filter size,  $c_B$  the number of channels in input  $B$  and  $n$  the number of filters.  $d$  is equal to 1 for dynamic convolution and  $h \times w$  for dynamic local filtering, which we discuss below. The filters are applied to input  $I_B \in \mathbb{R}^{h \times w \times c_B}$  to generate an output  $G = \mathcal{F}_\theta(I_B)$ , with  $G \in \mathbb{R}^{h \times w \times n}$ . The filter size  $s$  determines the receptive field and is chosen depending on the application. The size of the receptive field can also be increased by stacking multiple dynamic filter modules. This is for example useful in applications that may involve large local displacements.

The filter-generating network can be implemented with any differentiable architecture, such as a multilayer perceptron or a convolutional network. A convolutional network is particularly suitable when using images as input to the filter-generating network.

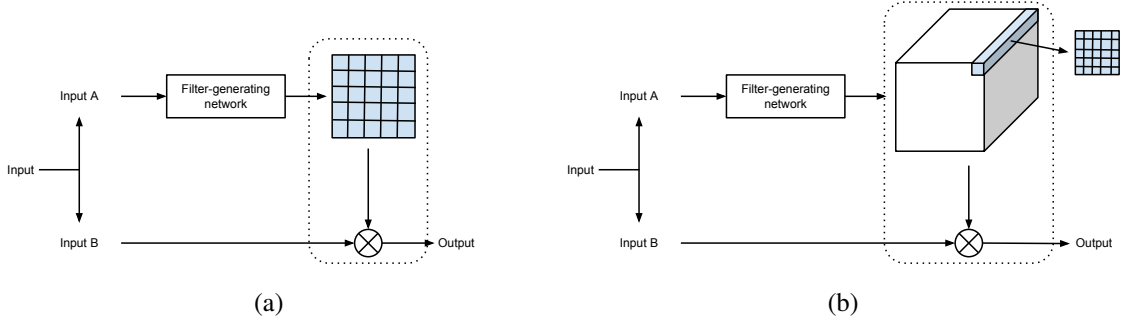


Figure 2: *Left*: Dynamic convolution: the filter-generating network produces a single filter that is applied convolutionally on  $I_B$ . *Right*: Dynamic local filtering: each location is filtered with a location-specific dynamically generated filter.

### 3.2 Dynamic Filtering Layer

The dynamic filtering layer takes images or feature maps  $I_B$  as input and outputs the filtered result  $G \in \mathbb{R}^{h \times w \times n}$ . For simplicity, in the experiments we only consider a single feature map ( $c_B = 1$ ) filtered with a single generated filter ( $n = 1$ ), but this is not required in a general setting. The dynamic filtering layer can be instantiated as a dynamic convolutional layer or a dynamic local filtering layer.

**Dynamic convolutional layer.** A dynamic convolutional layer is similar to a traditional convolutional layer in that the same filter is applied at every position of the input  $I_B$ . But different from the traditional convolutional layer where filter weights are model parameters, in a dynamic convolutional layer the filter parameters  $\theta$  are dynamically generated by a filter-generating network:

$$G(i, j) = \mathcal{F}_\theta(I_B(i, j)) \quad (1)$$

The filters are sample-specific and conditioned on the input of the filter-generating network. The dynamic convolutional layer is shown schematically in Figure 2(a). Given some prior knowledge about the application at hand, it is sometimes possible to facilitate training by constraining the generated convolutional filters in a certain way. For example, if the task is to produce a translated version of the input image  $I_B$  where the translation is conditioned on another input  $I_A$ , the generated filter can be sent through a softmax layer to encourage a spiked filter with most elements set to zero. We can also make the filter separable: instead of a single square filter, generate separate horizontal and vertical filters that are applied to the image consecutively similar to what is done in [13].

**Dynamic local filtering layer.** An extension of the dynamic convolution layer that proves interesting, as we show in the experiments, is the dynamic local filtering layer. In this layer the filtering operation is not translation invariant anymore. Instead, different filters are applied to different positions of the input  $I_B$  similarly to the traditional locally connected layer: for each position  $(i, j)$  of the input  $I_B$ , a specific local filter  $\mathcal{F}_\theta^{(i, j)}$  is applied to the region centered around  $I_B(i, j)$ :

$$G(i, j) = \mathcal{F}_\theta^{(i, j)}(I_B(i, j)) \quad (2)$$

The filters used in this layer are not only sample specific but also position specific. Note that dynamic convolution as discussed in the previous section is a special case of local dynamic filtering where the local filters are shared over the image’s spatial dimensions. The dynamic local filtering layer is shown schematically in Figure 2b. If the generated filters are again constrained with a softmax function so that each filter only contains one non-zero element, then the dynamic local filtering layer replaces each element of the input  $I_B$  by an element selected from a local neighbourhood around it. This offers a natural way to model local spatial deformations conditioned on another input  $I_A$ . The dynamic local filtering layer can perform not only a single transformation like the dynamic convolutional layer, but also position-specific transformations like local deformation. Before or after applying the dynamic local filtering operation we can add a dynamic pixel-wise bias to each element of the input  $I_B$  to address situations like photometric changes. This dynamic bias can be produced by the same filter-generating network that generates the filters for the local filtering.

When inputs  $I_A$  and  $I_B$  are both images, a natural way to implement the filter-generating network is with a convolutional network. This way, the generated position-specific filters are conditioned on the

local image region around their corresponding position in  $I_A$ . The receptive field of the convolutional network that generates the filters can be increased by using an encoder-decoder architecture. We can also apply a smoothness penalty to the output of the filter-generating network, so that neighboring filters are encouraged to apply the same transformation.

Another advantage of the dynamic local filtering layer over the traditional locally connected layer is that we do not need so many model parameters. The learned model is smaller and this is desirable in embedded system applications.

### 3.3 Relationship with other networks

The generic formulation of our framework allows to draw parallels with other networks in the literature. Here we discuss the relation with the spatial transformer networks [11], the deep stereo network [5, 23], and the residual networks [8, 10].

**Spatial Transformer Networks** The proposed dynamic filter network shares the same philosophy as the spatial transformer network proposed by [11], in that it applies a transformation conditioned on an input to a feature map. The spatial transformer network includes a localization network which takes a feature map as input, and it outputs the parameters of the desired spatial transformation. A grid generator and sampler are needed to apply the desired transformation to the feature map. This idea is similar to our dynamic filter network, which uses a filter-generating network to compute the parameters of the desired filters. The filters are applied on the feature map with a simple filtering operation that only consists of multiplication and summation operations.

A spatial transformer network is naturally suited for global transformations, even sophisticated ones such as a thin plate spline. The dynamic filter network is more suitable for local transformations, because of the limited receptive field of the generated filters, although this problem can be alleviated with larger filters, stacking multiple dynamic filter modules, and using multi-resolution extensions. A more fundamental difference is that the spatial transformer is only suited for spatial transformations, whereas the dynamic filter network can apply more general ones (e.g. photometric, filtering), as long as the transformation is implementable as a series of filtering operations. This is illustrated in the first experiment in the next section.

**Deep Stereo** The deep stereo network of [5] can be seen as a specific instantiation of a dynamic filter network with a local filtering layer where inputs  $I_A$  and  $I_B$  denote the same image, only a horizontal filter is generated and softmax is applied to each dynamic filter. The effect of the selection tower used in their network is equivalent to the proposed dynamic local filtering layer. For the specific task of stereo prediction, they use a more complicated architecture for the filter-generating network.

**Residual Networks** We can also draw some parallels with the recently introduced residual networks [8, 10]. The relation between residual networks and dynamic filter networks becomes clear when we redraw the diagram of our architecture (see Figure 3). The core idea of ResNet is to learn a residual function with respect to the identity mapping, which is implemented as an additive shortcut connection. In the dynamic filter network, we also have two branches where one branch acts as a shortcut connection. However, instead of merging the output of the two branches with addition, we merge them with a dynamic filtering layer which is multiplicative in nature.

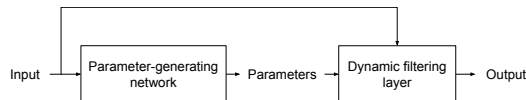


Figure 3: Relation with residual networks.

## 4 Experiments

The Dynamic Filter Network can be used in different ways in a wide variety of applications. In this section we show its application in learning steerable filters, video prediction and also stereo prediction. The first application shows a simple use case of a dynamic filter network which uses a dynamic convolutional layer with two different types of inputs. The second one shows that we can integrate the dynamic filter module with a dynamic local filtering layer in a recurrent network to predict a sequence of frames. The third one shows its use case when there is only one kind of input. We use *Theano* [2] based library *Lasagne* [3] to implement all the experiments.

Model	Moving MNIST	
	# params	bce
FC-LSTM [21]	142,667,776	341.2
Conv-LSTM [20]	7,585,296	367.1
DFN (ours)	<b>637,361</b>	<b>285.2</b>

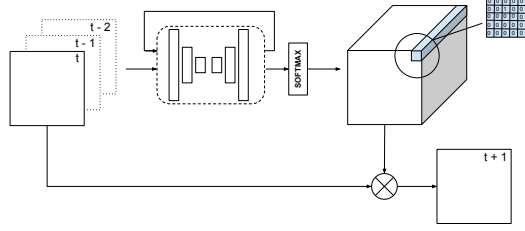


Table 1: *Left*: Quantitative results on Moving MNIST: number of model parameters and average binary cross-entropy (bce). *Right*: The dynamic filter network for video prediction.

#### 4.1 Learning steerable filters

We first set up a simple experiment to illustrate the basics of the dynamic filter module with a dynamic convolution layer. The task is to filter an input image with a steerable filter of a given orientation  $\theta$ . The network must learn this transformation from looking at input-output pairs, consisting of randomly chosen input images and angles together with their corresponding output.

The task of the filter-generating network here is to transform an angle into a filter, which is then applied to the input image to generate the final output. We implement the filter-generating network as a few fully-connected layers with the last layer containing 81 neurons, corresponding to the elements of a 9x9 convolution filter. Figure 4 shows an example of the trained network. It has indeed learned the expected filters and applies the correct transformation to the image.

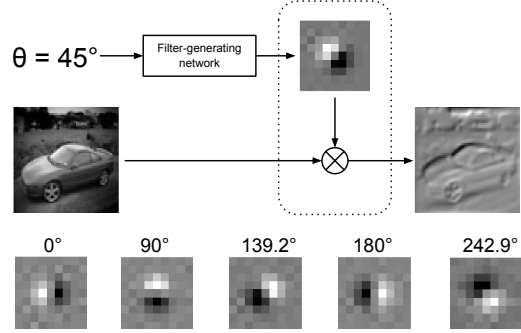


Figure 4: The dynamic filter network for learning steerable filters and several examples of learned filters.

#### 4.2 Video prediction

Here we describe how we make use of the proposed dynamic filter network for video prediction. The architecture of our model is shown in Table 1 (right). Given a sequence of frames, the task is to predict the sequence of future frames that directly follow the input frames. To address this task we use the convolutional encoder-decoder as the filter-generating network where the encoder consists of several strided convolutional layers and the decoder consists of several unpooling layers and convolutional layers. The convolutional encoder-decoder is able to exploit the spatial correlation within a frame and generates feature maps that are of the same size as the frame. To exploit the temporal correlation between frames we add a recurrent connection inside the filter-generating network: we pass the previous hidden state through two convolutional layers and take the sum with the output of the encoder to produce the new hidden state. During prediction, we propagate the prediction from the previous time step. Note that we use a very simple recurrent architecture rather than the more advanced LSTM as in [21, 20]. A softmax layer is applied to each generated filter such that each filter is encouraged to have only a few non-zero elements. To produce the prediction of the next frame, the generated filters are applied on the previous frame to transform it according to the dynamic local filtering mechanism explained in Section 3. The use of a softmax layer helps the dynamic filtering layer to generate sharper images because each pixel in the output image comes from only a few pixels in the previous frame.

**Moving MNIST** We first evaluate the method on the moving MNIST dataset [21]. We follow the setting in [21], that is, given a sequence of 10 frames with 2 moving digits as input, we predict the following 10 frames. We use the code provided by [21] to generate training samples on-the-fly, and test it on the provided test set for comparison. Only simple preprocessing is done to convert pixel values into the range [0,1].

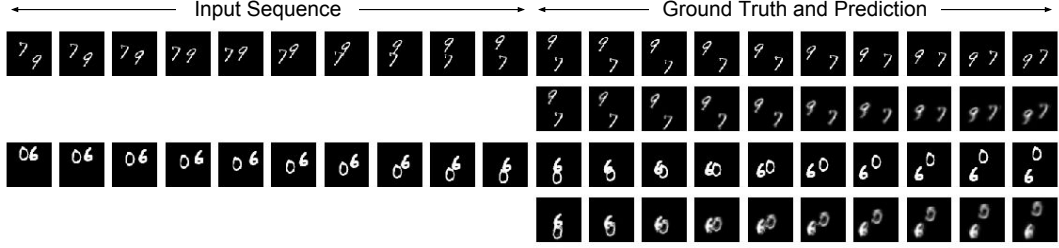


Figure 5: Qualitative results on moving MNIST. Note that the network has learned the bouncing dynamics and separation of overlapping digits. More examples and out-of-domain results are in the supplementary material.

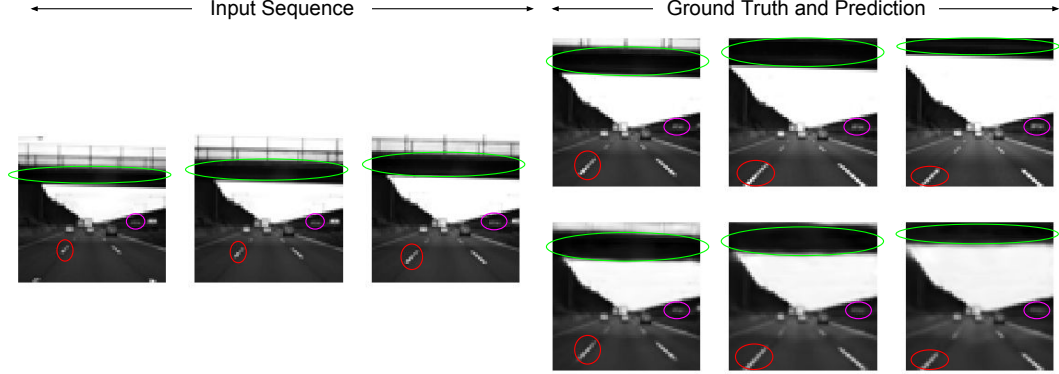


Figure 6: Qualitative results of video prediction on the Highway Driving dataset. Note the good prediction of the lanes (red), bridge (green) and a car moving in the opposite direction (purple).

We use the average binary cross-entropy over the 10 frames as loss function. The size of the dynamic filters is set to  $9 \times 9$ . We initialize all model parameters using the method proposed in [9] and use the Adam optimizer [12] with a learning rate of 0.001 to update those parameters. The network is trained end-to-end by backpropagation for 20,000 iterations with mini-batch size of 16. The quantitative results are shown in Table 1 (left). We use the cross-entropy of predictions as the evaluation metric. Our method outperforms the state-of-the-art [21, 20] and this with a much smaller model. Figure 5 shows some qualitative results. With the dynamic local filtering layer our method is able to correctly learn the individual motions of digits. The convolutional encoder-decoder has a large receptive field and this helps the model to learn the bouncing behavior and generate the right filters in case when digits bounce off the walls. We observe that the predictions deteriorate over time, i.e. the digits become blurry. This is partly because of the model error: our model is not able to perfectly separate digits after an overlap, and these errors accumulate over time. Another cause of blurring comes from an artifact of the dataset: because of imperfect cropping, it is uncertain when exactly the digit will bounce and change its direction. The behavior is not perfectly deterministic. This uncertainty combined with the pixel-wise loss function encourages the model to "hedge its bets" when a digit reaches the boundary, causing a blurry result. This issue could be alleviated with the methods proposed in [6, 7, 1].

**Highway Driving** We also evaluate this method on real-world data. From our industrial partner we obtained a video of a car driving on the highway. Compared to natural video like UCF101 used in [18, 14], the highway driving data is highly structured and much more predictable, making it a good testbed for video prediction. There are many cases with illumination changes such as when the car drives through a tunnel. To address this issue, we make a small modification to the architecture as shown in Table 1 (right) by adding a dynamic per-pixel bias before the filtering operation in the dynamic local filtering layer. Because the Highway Driving sequence is less deterministic than moving MNIST, we only predict the next 3 frames given an input sequence of 3 frames. For longer sequences, the uncertainty would become too high for the network to learn a reasonable prediction with a simple pixel-wise loss function. A sampling based method might alleviate this problem but we leave it as future work. We split the approximately 20,000 frames of the 30-minute video into a

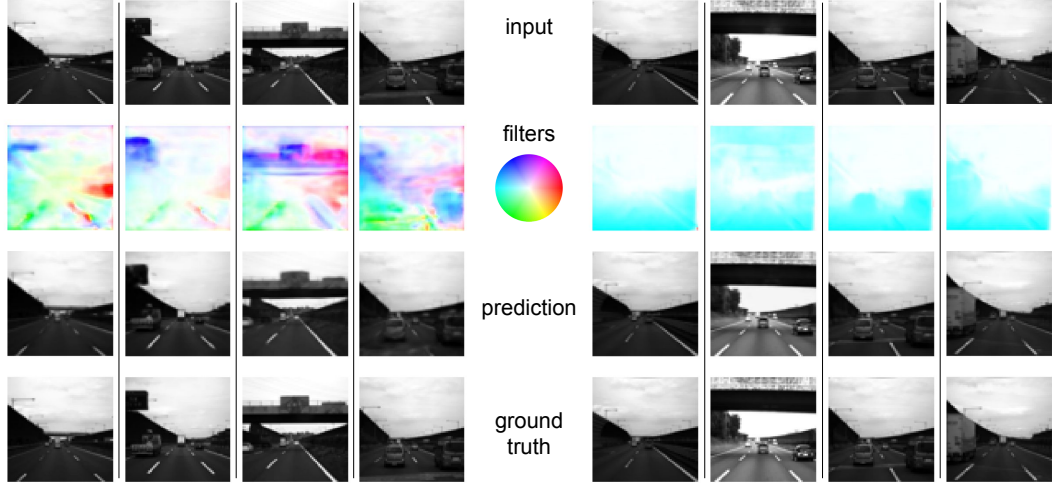


Figure 7: Some samples for video (*left*) and stereo (*right*) prediction and visualization of the dynamically generated filters. More examples and a video can be found in the supplementary material.

training set of 16,000 frames and a test set of 4,000 frames. During training, segments of 6 frames are selected randomly from the training set.

We train with a Euclidean loss function and obtain a loss of 13.54 on the test set with a model consisting of 368,122 parameters. Figure 6 shows some qualitative results. Similar to the experiment on moving MNIST, the predictions get blurry over time. This can partly be attributed to the increasing uncertainty combined with an element-wise loss-function which encourages averaging out the possible predictions. Moreover, the errors accumulate over time which after a while makes the network operate in an out-of-domain regime.

We also visualize the dynamically generated filters of the trained model, in a flow-like manner. For each element of a filter we compute its shift to the center in x-axis and y-axis. Taking the weighted sum of x-axis shifts over all filter elements, we can then get the overall x-axis shift caused by one filter. Similarly, we can get the overall y-axis shift. A filter can thus approximately be visualized as a 2-dimensional vector. We then visualize the filters in the same way as optical flow, see Figure 7 (left). Though the flow map is not that smooth, this byproduct is learned in an unsupervised way by only training on unlabeled video data which is different from e.g. [4].

### 4.3 Stereo prediction

We also apply the Dynamic Filtering Network to the task of stereo prediction, which we define as predicting the right view given the left view of two horizontal-disparity cameras. This task is a variant of video prediction, where the goal is to predict a new view in space rather than in time, and from a single image rather than multiple ones. Flynn *et al.* [5] developed a deep network for new view synthesis from multiple views in unconstrained settings like museums, parks and streets. We limit ourselves to the more structured Highway Driving dataset and a classical two-view stereo setup.

We recycle the architecture from the previous section, but drop the recurrent connection which is used to model temporal correlation. Besides, based on the assumption that corresponding points are on the same horizontal line, we replace the square 9x9 filters with horizontal 13x1 filters. The network is trained and evaluated on the same train- and test split as in the previous section but with the left view as input and the right one as target. It reaches a loss of 0.52 on the test set with a model consisting of 464,494 parameters. Some qualitative results are shown in Figure 7 (right). The network has learned to shift objects to the left depending on their distance to the camera.

We again compute flow-like maps for the generated dynamic filters. As shown in Figure 7 (right) the network has effectively learned to estimate depth information from a single image. The results suggest that it is possible to use the proposed dynamic filter network architecture to pre-train networks for optical flow and disparity map estimation in an unsupervised manner using only unlabeled data.



## 5 Conclusion

In this paper we introduced Dynamic Filter Networks, a class of networks that applies dynamically generated filters to an image in a sample-specific way. We discussed two versions: dynamic convolution and dynamic local filtering. We validated our framework in the context of steerable filters, video prediction and stereo prediction. As future work, we plan to explore the potential of dynamic filter networks on other tasks, such as finegrained image classification, where filters could learn to adapt to the object pose, or image deblurring, where filters can be tuned to adapt to the image structure.

## References

- [1] Hugo Larochelle Ole Winther Anders B. L. Larsen, Søren Kaae Sønderby. Autoencoding beyond pixels using a learned similarity metric. In *ICML*, 2016.
- [2] Frédéric Bastien, Pascal Lamblin, Razvan Pascanu, James Bergstra, Ian J. Goodfellow, Arnaud Bergeron, Nicolas Bouchard, and Yoshua Bengio. Theano: new features and speed improvements. Deep Learning and Unsupervised Feature Learning NIPS 2012 Workshop, 2012.
- [3] Sander Dieleman, Jan Schlüter, Colin Raffel, Eben Olson, Søren Kaae Sønderby, Daniel Nouri, Daniel Maturana, Martin Thoma, and Eric Battenberg. Lasagne: First release., August 2015.
- [4] Alexey Dosovitskiy, Philipp Fischer, Eddy Ilg, Philip Häusser, Caner Hazirbas, Vladimir Golkov, Patrick van der Smagt, Daniel Cremers, and Thomas Brox. Flownet: Learning optical flow with convolutional networks. In *ICCV*, 2015.
- [5] John Flynn, Ivan Neulander, James Philbin, and Noah Snavely. Deepstereo: Learning to predict new views from the world’s imagery. In *CVPR*, 2015.
- [6] Ian J. Goodfellow, Jean Pouget-Abadie, Mehdi Mirza, Bing Xu, David Warde-Farley, Sherjil Ozair, Aaron C. Courville, and Yoshua Bengio. Generative adversarial nets. In *NIPS*, 2014.
- [7] Ross Goroshin, Michaël Mathieu, and Yann LeCun. Learning to linearize under uncertainty. In *NIPS*, 2015.
- [8] Kaiming He, Xiangyu Zhang, Shaoqing Ren, and Jian Sun. Deep residual learning for image recognition. *CoRR*, abs/1512.03385, 2015.
- [9] Kaiming He, Xiangyu Zhang, Shaoqing Ren, and Jian Sun. Delving deep into rectifiers: Surpassing human-level performance on imagenet classification. In *ICCV*, 2015.
- [10] Kaiming He, Xiangyu Zhang, Shaoqing Ren, and Jian Sun. Identity mappings in deep residual networks. *CoRR*, abs/1603.05027, 2016.
- [11] Max Jaderberg, Karen Simonyan, Andrew Zisserman, and Koray Kavukcuoglu. Spatial transformer networks. In *NIPS*, 2015.
- [12] Diederik P. Kingma and Jimmy Ba. Adam: A method for stochastic optimization. *CoRR*, abs/1412.6980, 2014.
- [13] Benjamin Klein, Lior Wolf, and Yehuda Afek. A dynamic convolutional layer for short range weather prediction. In *CVPR*, 2015.
- [14] Michaël Mathieu, Camille Couprie, and Yann LeCun. Deep multi-scale video prediction beyond mean square error. 2016.
- [15] Hyeonwoo Noh, Paul Hongsuck Seo, and Bohyung Han. Image question answering using convolutional neural network with dynamic parameter prediction. In *CVPR*, 2016.
- [16] Junhyuk Oh, Xiaoxiao Guo, Honglak Lee, Richard L. Lewis, and Satinder P. Singh. Action-conditional video prediction using deep networks in atari games. In *NIPS*, 2015.
- [17] Viorica Patraucean, Ankur Handa, and Roberto Cipolla. Spatio-temporal video autoencoder with differentiable memory. *CoRR*, abs/1511.06309, 2015.
- [18] Marc’Aurelio Ranzato, Arthur Szlam, Joan Bruna, Michaël Mathieu, Ronan Collobert, and Sumit Chopra. Video (language) modeling: a baseline for generative models of natural videos. *CoRR*, abs/1412.6604, 2014.
- [19] Gernot Riegler, Samuel Schulter, Matthias Rütger, and Horst Bischof. Conditioned regression models for non-blind single image super-resolution. In *ICCV*, 2015.
- [20] Xingjian Shi, Zhouong Chen, Hao Wang, Dit-Yan Yeung, Wai-Kin Wong, and Wang-chun Woo. Convolutional LSTM network: A machine learning approach for precipitation nowcasting. In *NIPS*, 2015.
- [21] Nitish Srivastava, Elman Mansimov, and Ruslan Salakhutdinov. Unsupervised learning of video representations using lstms. In *ICML*, 2015.

- [22] Rupesh Kumar Srivastava, Klaus Greff, and Jürgen Schmidhuber. Training very deep networks. In *NIPS*, 2015.
- [23] Junyuan Xie, Ross Girshick, and Ali Farhadi. Deep3d: Fully automatic 2d-to-3d video conversion with deep convolutional neural networks. *arXiv preprint arXiv:1604.03650*, 2016.
- [24] Jimei Yang, Scott Reed, Ming-Hsuan Yang, and Honglak Lee. Weakly-supervised disentangling with recurrent transformations for 3d view synthesis. In *NIPS*, 2015.
- [25] Junho Yim, Heechul Jung, ByungIn Yoo, Changkyu Choi, Du-Sik Park, and Junmo Kim. Rotating your face using multi-task deep neural network. In *CVPR*, 2015.

## A Video Prediction

In this section, we add more results of the experiments on the moving MNIST and highway driving datasets. For the moving MNIST experiment, we also visualize the dynamically generated filter for the first predicted frame in Figure 9. We also run the model which is trained on 2 moving digits on out-of-domain data which has 1 moving digit or 3 moving digits, which shows the generalization ability of the learned model. The result is shown in Figure 10. It shows the model has good generalization ability. We added an animated gif-file for every sequence and those can be found online: [https://drive.google.com/file/d/0B2k\\_yg56pxkxVFFWMDVycXg3Qmc/view?usp=sharing](https://drive.google.com/file/d/0B2k_yg56pxkxVFFWMDVycXg3Qmc/view?usp=sharing).

### A.1 Moving MNIST

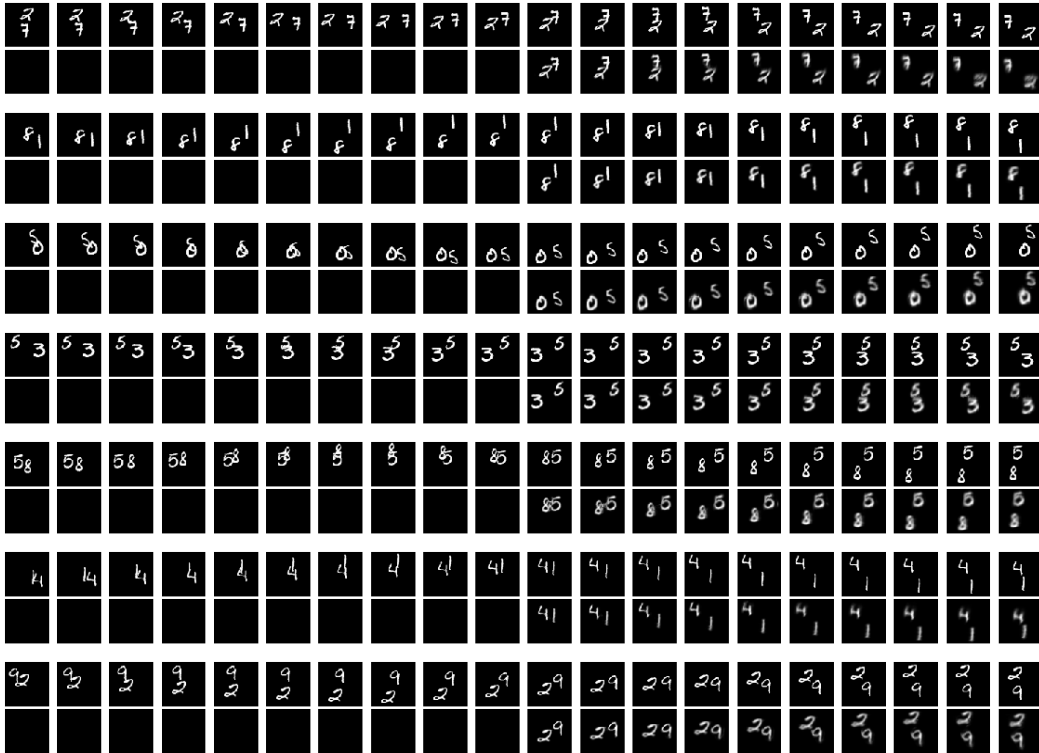


Figure 8: Results on moving MNIST dataset with 2 moving digits. In the first row, the left half are input sequence and the right half are ground truth of the future frames; in the second row, the right half is the prediction of our model.

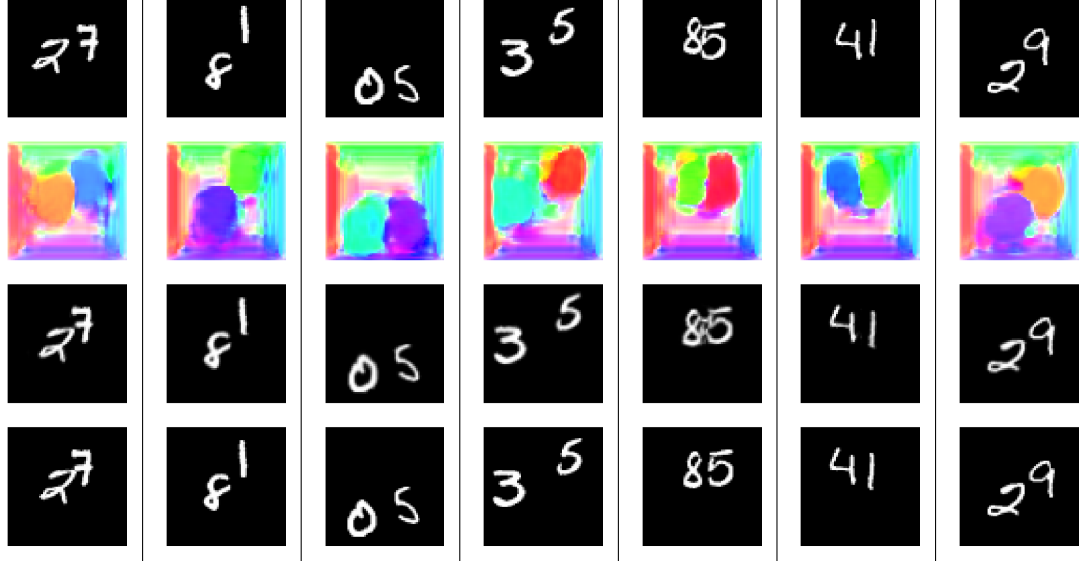


Figure 9: Visualization of the dynamically generated filters. The first row are the previous frame, the second row are the visualization of filters, the third row are our prediction of the current frame and the fourth row are the ground truth.

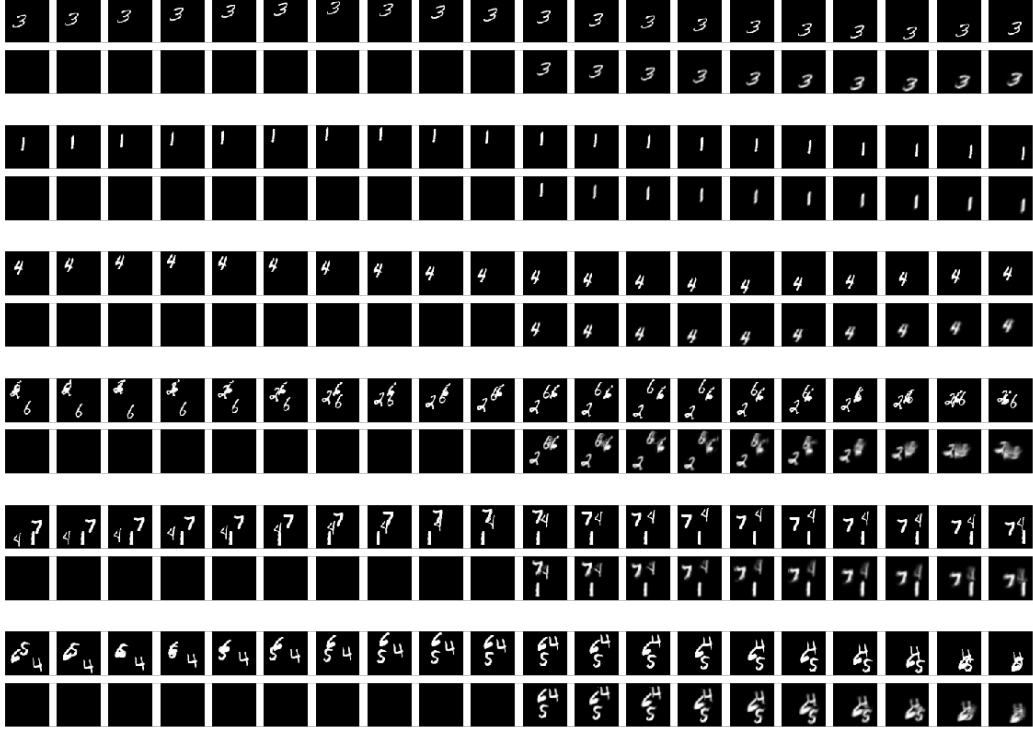


Figure 10: Results of out-of-domain input experiment with 1 moving digit and 3 moving digits.

## A.2 Highway driving

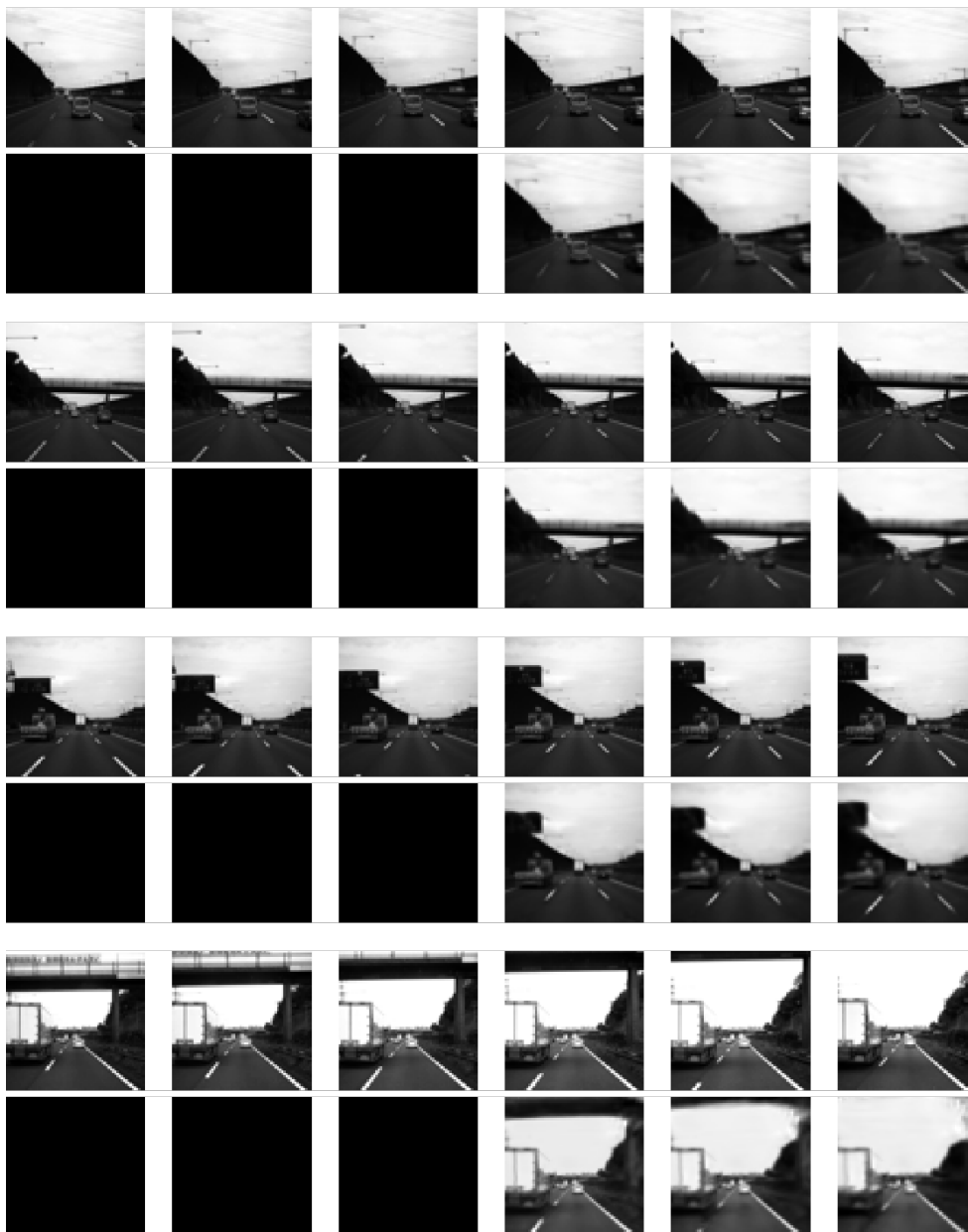


Figure 11: Results on highway driving dataset.

## B Stereo Prediction

We make a video of stereo prediction results for the whole test sequence which can be found at [https://drive.google.com/file/d/0B2k\\_yg56pxkxVFFWMDVycXg3Qmc/view?usp=sharing](https://drive.google.com/file/d/0B2k_yg56pxkxVFFWMDVycXg3Qmc/view?usp=sharing). In each frame, the first one is the left view image, the second one is the visualization of filters, the third one is our prediction of the right view, and the last one is the groundtruth.